

# $I = 1, J = 1$ resonances in the Padé unitarized $W_L^+ W_L^-$ scattering amplitude

Duane A. Dicus

Center for Particle Physics, University of Texas, Austin, Texas 78712

Wayne W. Repko

Department of Physics and Astronomy, Michigan State University, East Lansing, Michigan 48824

(Received 20 November 1992)

We show that the Padé unitarized  $I = 1, J = 1$  partial wave amplitude for  $W_L^+ W_L^-$  elastic scattering exhibits resonant behavior for relatively low values of the Higgs-boson mass parameter  $m_H$ . The  $p$ -wave resonance can occur when  $\sqrt{s} \gtrsim m_H$ . This is in contrast with the  $I = 0, J = 0$  resonance which occurs in the  $W_L^+ W_L^- - Z_L^0 Z_L^0$  system for  $\sqrt{s} \ll m_H$ . The observability of the  $I = 1$  resonance in high-energy  $pp$  collisions is examined.

PACS number(s): 13.85.Qk, 14.80.Er, 14.80.Gt

Recently, it has been shown [1-3] that the [1,1] Padé unitarized  $I = 0, J = 0$  partial wave amplitude for the  $W_L^+ W_L^- - Z_L^0 Z_L^0$  system exhibits a resonance of mass  $\mu$  with  $\mu \lesssim m_H$ . The width of this resonance decreases as  $m_H$  increases. For  $m_H \gtrsim 10$  TeV, the essential features of the resonant behavior can be obtained from the one-loop-corrected  $I = 0$   $s$ -wave amplitude  $c_{I=0}$  which is expressible as an expansion in powers of  $fs$  as [4, 5]

$$c_{I=0}(s) = fs + \frac{f^2 s^2}{2\pi} \left[ -\frac{25}{9} \ln\left(\frac{s}{m_H^2}\right) - \frac{3346}{108} + \frac{11\sqrt{3}}{2} \pi + 2\pi i \right], \quad (1)$$

$$= c_{I=0}^{(1)} + c_{I=0}^{(2)}. \quad (2)$$

Here  $f$  denotes

$$f = \pi \frac{1}{(4\pi v_0)^2}, \quad (3)$$

and  $v_0$ , the Higgs-field vacuum expectation value, is given by

$$v_0^2 = \frac{4m_W^2}{g^2}. \quad (4)$$

The [1,1] Padé approximant for this amplitude is

$$c_{I=0}^{[1,1]} = \frac{c_{I=0}^{(1)2}}{c_{I=0}^{(1)} - c_{I=0}^{(2)}}. \quad (5)$$

Using the fact that, for eigenamplitudes, perturbative unitarity relates the imaginary part of the one-loop correction to the square of the Born contribution, we can write

$$c_{I=0}^{[1,1]} = \frac{c_{I=0}^{(1)2}}{c_{I=0}^{(1)} - \text{Rec}_{I=0}^{(2)} - ic_{I=0}^{(1)2}}. \quad (6)$$

For resonances which are sufficiently narrow, the resonant mass  $\mu$  can be determined by the requirement that

the real part of the denominator in Eq. (6) vanish at  $\sqrt{s} = \mu$ . The expressions for the resonance mass  $\mu$  and its width  $\Gamma(\mu)$  given in Refs. [1, 2] can be obtained by expanding  $c_{I=0}^{(1)}(s) - \text{Rec}_{I=0}^{(2)}(s)$  about the point  $s = \mu^2$ .

From earlier investigations of unitarity effects in  $\pi\pi$  scattering [6, 7], the existence of an  $I = 1$   $p$ -wave resonance in the unitarized  $W_L^+ W_L^- \rightarrow W_L^+ W_L^-$  amplitude of the standard model is not entirely unexpected. The difference between the  $I = 0$  and  $I = 1$  cases is that the  $s \ll m_H^2$  limit analogous to Eq. (1) cannot be used to analyze the  $I = 1$  resonance [8]. For this channel, the corresponding expression is

$$c_{I=1} = \frac{fs}{6} + \frac{f^2 s^2}{2\pi} \left[ \frac{143}{54} - \frac{\sqrt{3}}{2} \pi + \frac{\pi}{18} i \right], \quad s \ll m_H^2. \quad (7)$$

Not only is Eq. (7) independent of  $m_H$ , but the real part of the associated Padé denominator,

$$c_{I=1}^{(1)}(s) - \text{Rec}_{I=1}^{(2)}(s) = \frac{fs}{6} - \frac{f^2 s^2}{2\pi} \left[ \frac{143}{54} - \frac{\sqrt{3}}{2} \pi \right], \quad (8)$$

is positive definite. Consequently, there is no resonance in this limit.

In order to determine if there is a  $p$ -wave resonance for  $s \sim m_H^2$ , it is necessary to examine the  $I = 1$  version of Eq. (6) using

$$c_{I=1}^{(1)}(s) = -\frac{g^2 m_H^4}{64\pi m_W^2 s} \left[ 2 - \left( 1 + \frac{2m_H^2}{s} \right) \ln \left( 1 + \frac{s}{m_H^2} \right) \right], \quad (9)$$

together with the complete expression for  $\text{Rec}_{I=1}^{(2)}(s)$  [4]. In Figs. 1 and 2, we plot the Padé unitarized  $I = 1$  amplitude for several values of  $m_H$ . The peak in the amplitude represents a true resonance in the sense that the Argand diagram exhibits the expected resonant behavior. For

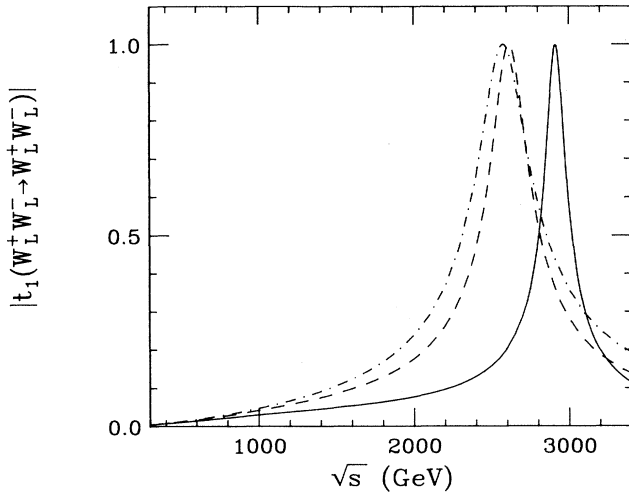
p-wave  $W_L^+ W_L^- \rightarrow W_L^+ W_L^-$  Amplitude

FIG. 1. The Padé unitarized  $p$ -wave amplitude  $t_1(W_L^+ W_L^- \rightarrow W_L^+ W_L^-)$  is plotted for  $m_H = 1$  TeV (solid), 1.5 TeV (dashed), and 2 TeV (dash-dotted).

relatively low values of  $m_H \lesssim 1$  TeV, the resonance is narrow and occurs at a mass  $\mu \gtrsim 3$  TeV. As  $m_H$  increases to about 2 TeV,  $\mu$  decreases to a minimum value of 2.6 TeV. Further increases in  $m_H$  yield an increasing value of  $\mu$  and an increasing width  $\Gamma(m_H)$ . The behavior of the resonant mass and its width as a function of  $m_H$  is summarized in Fig. 3. Also shown as a dashed line is the mass of the  $I = 0, J = 0$  resonance for the same range of  $m_H$  [1]. The  $J = 1$  resonance persists even for low values of  $m_H$  whereas the  $J = 0$  resonance occurs at  $\mu = m_H$  for  $m_H$  sufficiently small. For example, when  $m_H = 500$  GeV, the  $J = 1$  resonance occurs at  $\mu = 4$  TeV with an extremely narrow width of about 30 GeV. Any discussion of resonances deduced from a Padé unitarized amplitude must be examined to determine if

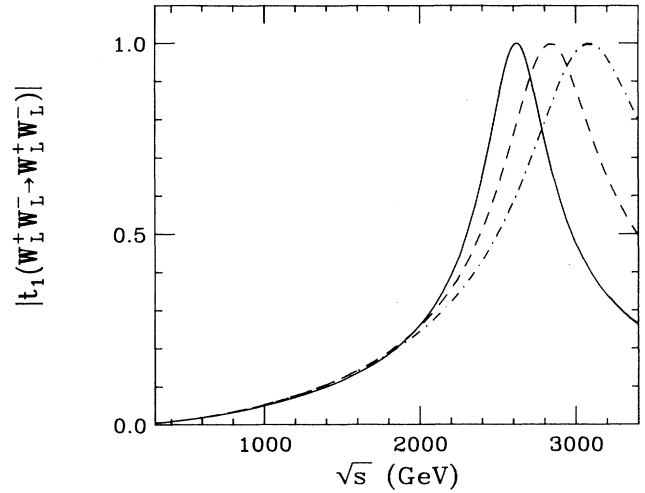
p-wave  $W_L^+ W_L^- \rightarrow W_L^+ W_L^-$  Amplitude

FIG. 2. Same as Fig. 1 with  $m_H = 2.5$  TeV (solid), 3.75 TeV (dashed), and 5 TeV (dash-dotted).

the resonances are located in a region of  $s$  for which the scheme is sensible. This point is treated in some detail in Ref. [9], which obtains results similar to those presented here. Finally, we note that higher partial waves also exhibit resonant behavior. The  $J = 3$  partial wave has a resonance at  $\mu = 7.4$  TeV for  $m_H = 1$  TeV, and when  $m_H = 500$  GeV  $\mu$  exceeds 10 TeV.

We have explored the observability of the  $p$ -wave resonance at energies reached at the Superconducting Super Collider (SSC) by computing the  $W$ -pair invariant mass distribution for the process  $pp \rightarrow W_L^+ W_L^- X$  using the effective  $W$  approximation [10–12]. When the quark and vector boson distribution functions  $f$  and  $\hat{f}$  are included, the expression for the invariant mass distribution with contributions from the  $s$  and  $p$  waves is

$$\frac{d\sigma}{dm_{WW}} = \frac{64\pi}{s} \int_{\tau_{\min}}^1 \frac{d\tau}{\tau} \int_{-y_0}^{y_0} dy f(\sqrt{\tau}e^y) f(\sqrt{\tau}e^{-y}) \int_{-\hat{y}_0}^{\hat{y}_1} d\hat{y} \hat{f}(\sqrt{\hat{\tau}}e^{\hat{y}}) \hat{f}(\sqrt{\hat{\tau}}e^{-\hat{y}}) \left( \frac{z_0 |t_0|^2 + 3z_0^3 |t_1|^2}{m_{WW}} \right), \quad (10)$$

where

$$\tau_{\min} = \frac{m_{WW}^2}{s}, \quad \hat{\tau} = \frac{\tau_{\min}}{\tau}. \quad (11)$$

In Eq. (10),  $t_0 = \frac{2}{3} c_{I=0}^{[1,1]} + \frac{1}{3} c_{I=2}^{[1,1]}$ ,  $t_1 = c_{I=1}^{[1,1]}$ , and we have included a factor of 2 for the symmetry of the quark distributions in  $pp$  collisions. The integration limits  $y_0$ ,  $\hat{y}_0$ , and  $\hat{y}_1$  are a result of imposing a rapidity cut  $\eta_C$  on both of the final vector bosons. These limits are related to  $\eta_C$ ,  $\eta = \ln(1/\sqrt{\tau})$ , and  $\hat{\eta} = \ln(1/\sqrt{\hat{\tau}})$  as

$$\begin{aligned} y_0 &= \min(\eta, \eta_C + \hat{\eta}), \quad \hat{y}_0 = \min(\hat{\eta}, \eta_C + y), \\ \hat{y}_1 &= \min(\hat{\eta}, \eta_C - y). \end{aligned} \quad (12)$$

The value of  $z_0$ , which occurs in the range of the

$d(\cos\theta)$  integration, is determined by

$$z_0 = \min\left(\frac{1}{\beta} \tanh(\eta_C - |y + \hat{y}|), 1\right), \quad (13)$$

where  $\beta = \sqrt{1 - 4m_W^2/m_{WW}^2}$ . The vector boson distribution function  $\hat{f}(x)$  used in evaluating Eq. (10) corresponds to the distribution of longitudinal  $W$ 's,

$$\hat{f}_L(x) = \frac{\alpha_W}{4\pi} \frac{(1-x)}{x}, \quad (14)$$

and the quark distribution functions  $f(x)$  are the Bologna-CERN-Dubna-Munich-Saclay (BCDMS) fit of Harriman *et al.* [13].

Figures 4–6 show the results for  $d\sigma/dm_{WW}$  when  $m_H = 1, 2,$  and 5 TeV, respectively. Even for the low-

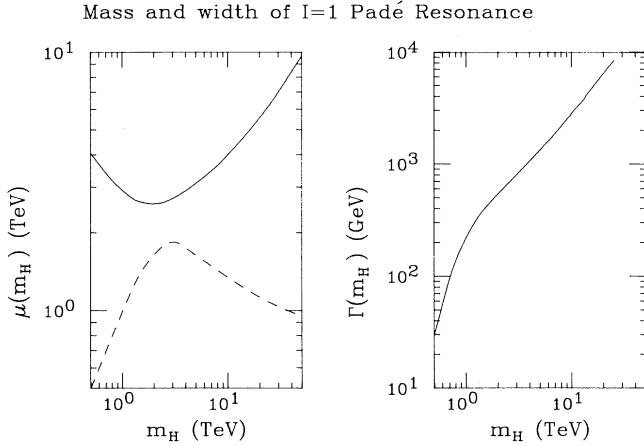


FIG. 3. The mass and width of the  $p$ -wave resonance are plotted as a function of  $m_H$ . The dashed line in the left-hand graph is a plot of the mass of the  $I = 0, J = 0$  resonance.

est resonance mass, corresponding to  $m_H \sim 2$ , the cross sections are not large. However, for an SSC luminosity of  $10^4 \text{ pb}^{-1}/\text{year}$ , the area between  $m_{WW}$  of 2400 and 2800 GeV contains an excess of about 75 events/year above a  $q\bar{q}$  background of 140 events/year. The same area for an integrated luminosity of  $10^5 \text{ pb}^{-1}/\text{year}$  attained at the CERN Large Hadron Collider (LHC) has approximately 23 extra events above a 220 event/year background. For  $m_H = 1 \text{ TeV}$ , the resonance is very narrow and occurs at a relatively large value of  $m_{WW}$  where the magnitude of the cross section is smaller. There are about 16 extra SSC events/year between  $m_{WW}$  equal 2800 and 3000 GeV out of a total number of events, including background, of 58. Thus, it seems unlikely that the  $J = 1$  resonance can be seen for  $m_H$  values much smaller than 1 TeV.

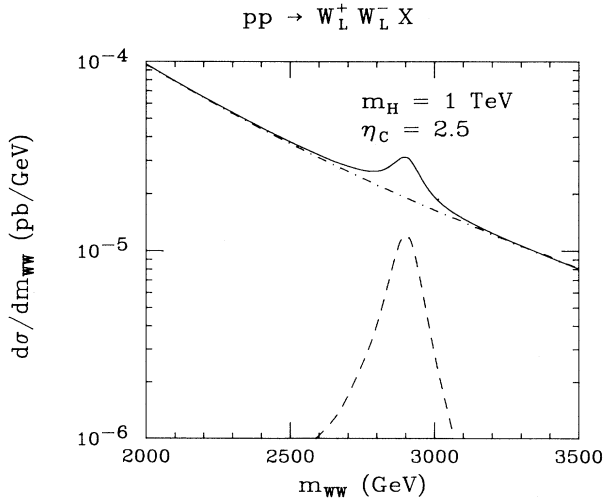


FIG. 4. The invariant mass distribution for the production of  $W_L^+ W_L^-$  pairs at an SSC energy of 40 TeV is plotted for  $m_H = 1 \text{ TeV}$ . The dashed line is the contribution from  $W_L^+ W_L^-$  scattering, the dash-dotted line the contribution from  $q\bar{q} \rightarrow W_L^+ W_L^-$ , and the total is given by the solid line. A rapidity cut  $\eta_C = 2.5$  is imposed on both  $W$ 's.

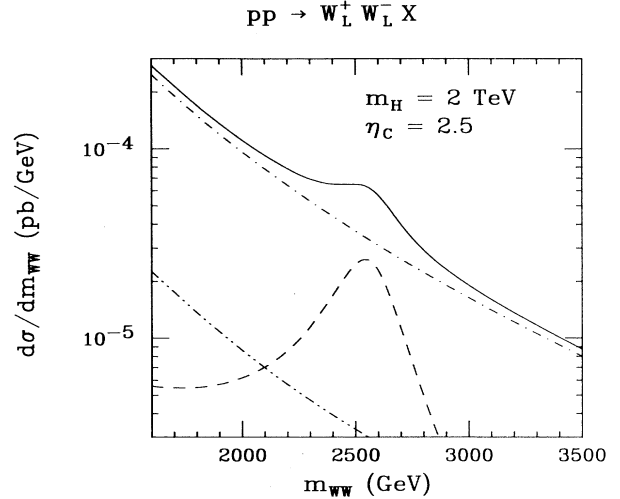


FIG. 5. Same as Fig. 4 except that  $m_H = 2 \text{ TeV}$ . The dashed-double-dotted line is the contribution of the  $s$ -wave resonance in this region of  $W_L^+ W_L^-$  invariant mass.

For  $m_H$  larger than 2 TeV the width of the resonance increases, which helps compensate for the somewhat smaller cross section. Thus Fig. 6 shows an excess of 38 events/year for  $m_{WW}$  from 2800 to 3200 GeV compared to 108 background events. Thus if data can be collected over a broad range of invariant mass it may be possible to detect the  $J = 1$  resonance even if  $m_H$  is larger than 5 TeV.

Our results for the signals one might expect in the  $I = 1, J = 1$   $W_L^+ W_L^- \rightarrow W_L^+ W_L^-$  channel are indicative of the observability of a  $p$ -wave resonance. The other  $I = 1$  channels,  $W_L^\pm Z_L^0 \rightarrow W_L^\pm Z_L^0$ , are potentially better candidates from the experimental point of view since they can be more completely reconstructed. Although their  $p$ -wave amplitudes are the same as those in the neutral channel, differences in the  $W_L^\pm Z_L^0$  luminosity and the  $q\bar{q}$  background require a complete calculation to determine the magnitude of the expected signals in these channels.

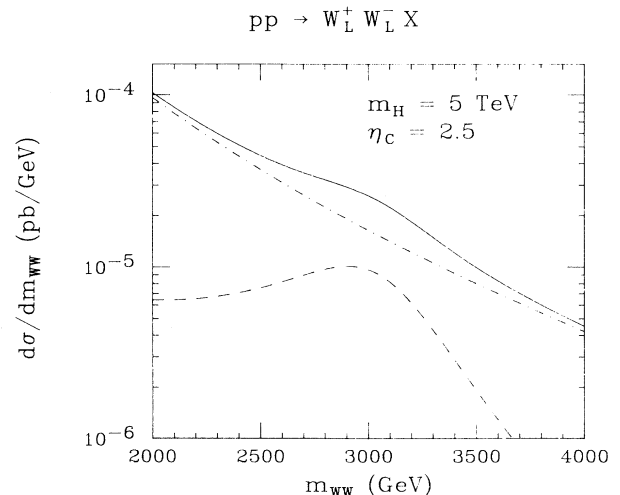


FIG. 6. Same as Fig. 4 except that  $m_H = 5 \text{ TeV}$ .

In summary the Padé amplitude for  $W_L^+ W_L^- \rightarrow W_L^+ W_L^-$  has resonances for  $J$  larger than zero as one might anticipate [6, 7]. We have studied the  $p$ -wave resonance determining its position and width for a broad range of possible values of the Higgs-boson mass parameter  $m_H$ . We have also calculated the production cross section in  $pp$  collisions and find that the resonance should be observable if  $m_H$  is larger than 1 TeV up to an  $m_H$  value somewhere above 5 TeV. This region of  $m_H$  corresponds to a resonance position between 2.6 and 3.2 TeV.

*Note added.* After the circulation of the unpublished version of this paper [University of Texas, Center for

Particle Physics DOE-ER40200-267 (1991)] we became aware of a paper by Atkinson, Harada, and Sanda [9], which reaches similar conclusions.

One of us (W.W.R.) wishes to thank G. Farrar for a useful communication. We would also like to thank Scott Willenbrock for helpful conversations. This research was supported in part by the National Science Foundation under Grant No. 90-06117 and by the U.S. Department of Energy under Contract No. DE-FG02-85ER40200. Computing resources were provided by the University of Texas Center for High Performance Computing.

- 
- [1] D. A. Dicus and W. W. Repko, Phys. Rev. D **42**, 3660 (1990).
  - [2] A. Dobado, M. J. Herrero, and T. N. Truong, Phys. Lett. B **235**, 129 (1990); **235**, 134 (1990); A. Dobado, *ibid.* **237**, 457 (1990).
  - [3] C. B. Chiu, E. C. G. Sudarshan, and G. Bhamathi, University of Texas Report No. DOE-ER40200-252, 1991 (unpublished).
  - [4] S. Dawson and S. S. D. Willenbrock, Phys. Rev. Lett. **62**, 1232 (1989); Phys. Rev. D **40**, 2880 (1989).
  - [5] M. Veltman and F. Yndurian, Nucl. Phys. **B325**, 1 (1989).
  - [6] L. S. Brown and R. L. Goble, Phys. Rev. Lett. **20**, 346 (1968).
  - [7] J. S. Basdevant and B. W. Lee, Phys. Rev. D **2**, 1680 (1970).
  - [8] The behavior of the Padé unitarized  $p$ -wave amplitude in this limit is also discussed by A. Dobado, M. J. Herrero, and J. Terron, Z. Phys. C **50**, 205 (1991); R. S. Willey, Phys. Rev. D **44**, 3646 (1991); and H. Veltman and M. Veltman, Acta Phys. Pol. B **22**, 669 (1991).
  - [9] D. Atkinson, M. Harada, and A. I. Sanda, Phys. Rev. D **46**, 3884 (1992).
  - [10] M. S. Chanowitz and M. K. Gaillard, Phys. Lett. **142B**, 85 (1984).
  - [11] G. L. Kane, W. W. Repko, and W. B. Rolnick, Phys. Lett. **148B**, 367 (1984).
  - [12] S. Dawson, Nucl. Phys. **B249**, 42 (1985).
  - [13] P. N. Harriman, A. D. Martin, W. J. Stirling, and R. G. Roberts, Phys. Rev. D **42**, 798 (1990).